GEORGIA INSTITUTE OF TECHNOLOGY
OFFICE OF CONTRACT ADMINISTRATION
SPONSORED PROJECT INITIATION

Date: April 4, 1979

Project Title: *Theory and Applications of High Resolution Spectra of Symmetric Polyatomic Molecules*

Project No: *G-41-676* Green card

Project Director: *Dr. William G. Harter*

Sponsor: *Research Corporation; New York, NY 10017*

Agreement Period: From *2/28/79* Until *All funds expended/Work conclude*

Type Agreement: *Grant/Check No. 6542 dated 2/26/79*

Amount: *$10,000.00*

Reports Required: *Annual Reports*

Sponsor Contact Person (s):

Technical Matters

R. Scott Pyron
Regional Director - Grants Program
Research Corporation
6075 Roswell Road, N.E.
Atlanta, Georgia 30328

Contractual Matters
(thru OCA)

Kendall W. King
Vice President - Grants Program
Research Corporation
405 Lexington Avenue
New York, NY 10017

Phone: (202) 599-5725

Defense Priority Rating: *none*

Assigned to: *Physics* (School/Laboratory)

COPIES TO:

Project Director
Division Chief (EES)
School/Laboratory Director
Dean/Director–EES
Accounting Office
Procurement Office
Security Coordinator (OCA)
Reports Coordinator (OCA)
Library, Technical Reports Section
EES Information Office
EES Reports & Procedures
Project File (OCA)
Project Code (GTRI)
Other

CA–3 (3/76)

GEORGIA INSTITUTE OF TECHNOLOGY OFFICE OF CONTRACT ADMINISTRATION

SPONSORED PROJECT TERMINATION SHEET

Date 6/25/82

Project Title: Theory & Applications of High Resolution Spectra of Symmetric Polyatomic Molecules

Project No: G-41-676

Project Director: Dr. William G. Harter

Sponsor: Research Corporation

Effective Termination Date: When funds are expended

Clearance of Accounting Charges: When funds are expended

Grant/Contract Closeout Actions Remaining:

None required.

- ☐ Final Invoice and Closing Documents
- ☐ Final Fiscal Report
- ☐ Final Report of Inventions
- ☐ Govt. Property Inventory & Related Certificate
- ☐ Classified Material Certificate
- ☐ Other _____

Assigned to: Physics (School/~~Laboratory~~)

COPIES TO:

~~Administrative Coordinator~~ RAN	~~Research Security Services~~	EES Public Relations (2)
Research Property Management	Reports Coordinator (OCA)	~~Computer Input~~
Accounting	Legal Services (OCA)	Project File
Procurement/EES Supply Services	Library	Other GTRI

FORM OCA 10:781

G-41-676

REPORT OF RESEARCH CORPORATION GRANT

(Please check one) (Submit original and one legible copy)

☐ Interim Report

☒ Terminal Report

INSTITUTION AND ADDRESS School of Physics
Georgia Institute of Technology
Atlanta Georgia 30332

PRINCIPAL INVESTIGATOR William G. Harter PHONE 894-5238

ACADEMIC RANK AND DEPARTMENT Associate Professor of Physics

SHORT TITLE OF RESEARCH SUPPORTED BY GRANT

Theory and Applications of High Resolution Spectra of Symmetric Polyatomic Molecules"

STARTING DATE Feb. 1977

SUMMARY OR PRINCIPAL FINDINGS AND THEIR SIGNIFICANCE (State succinctly in language understandable to one not necessarily expert in this field. Include extent to which original goals have been realized and any changes to original plan made or contemplated.)

(Attached)

EPORT OF RESEARCH CORPORATION GRANT
ige 2

'UDENT PARTICIPATION (Give names of students working on the project, their role in the research, their achievements and eir career plans.)

IPERS AND SCIENTIFIC TALKS (Give titles and references to papers or talks resulting from the work. Attach two copies of y reprints available, if not previously forwarded.)

heory of hyperfine and superfine levels in symmetric polyatomic molecules (I) Trigonal and trahedral molecules: Elementary spin 1/2 cases." Phys. Rev. A 19, 2277(1979)(Reprints hausted).

heory of hyperfine..(II)Elementary cases in octahedral hexafluoride molecules" Phys. Rev. A ,192(1981)(Reprints enclosed.)

roken unitary tableaus, itinerant nuclear spins, and spontaneous molecular symmetry collapse" the Unitary Group p.306,Lecture Notes in Chemistry,Editor J. Hinze Springer Verlag(1981).

HER SUPPORT (List amounts and sources—including institutional—of other contributions received or expected for this work.)

orgia Tech funds of $16,000 were matched to purchase HP9845 desk computer and plotter ov. 1980). As a result of the initial work a National Science Foundation Grant of 1,209 was awarded. (Jan. 1981-Jan. 1983).

PENDITURE OF RESEARCH CORPORATION GRANT FUNDS (The terminal report should be approved by an authorized officer the institution.)

a. Equipment, supplies (Itemize major expenditures)

$10,000 for HP9845 desk plotter system

b. Stipends (Academic status, rates, periods of appointment)

None

c. Other expenditures (Itemize and give purpose)

None

Jan 7 1981

ature of principal investigator — Date

ature of authorized officer of institution (required for terminal report only) — Date

and position of authorized officer of institution

The main achievement of the work concerns section (a) of the Research Corporation proposal to "provide analytical tools for new and more detailed laser spectra". The principal new results have almost exclusively focused on the sulfur hexafluoride SF_6 molecule since it is a prototype for the studies of laser isotope separation, principally, uranium enrichment schemes. The highest resolution and most detailed spectra have been the CO_2 laser saturation absorption spectra taken by Borde et. al.[1.] of the nuclear hyperfine structure in the 10 mm region of the ν_3 bands in SF_6. At first the experiment directions seemed distressing since the hyperfine structure of SF_6 is much more complicated than that of CF_4, SiF_4, and similar tetrahedral molecules. However, the theory of unitary and permutation tableaus was developed to provide a suprisingly simple description of the complex SF_6 states. Through this was gained an analytic basis for treating the hyperfine structure of most XF_n molecules.

The first new effect to be observed was spectral cluster-related "hyperfine mixing" between rovibronic spin species A_1, A_2, E, T_1, and T_2. In simpler molecules such as Hydrogen (H_2) the nuclear spin species "para"or A_1 and "ortho" or A_2 are very good stationary states,i.e. they do not "mix" readily. But in SF_6, CF_4, SiF_4, etc. the levels belonging to different species are clustered together so closely that nuclear spin-rotation interactions, however weak they may be, can exert a strong effect on the molecular eigenstates. In other words a weak effect gains an unexpected "leverage". For example we find using tableau notation that the A_{2u} and F_u spin species

$$|A_{2u}\rangle = \left|\begin{array}{|c|c|c|c|}\hline 1&2&3&4\\\hline 5&6\\\cline{1-2}\end{array}\right\rangle \quad \text{and,} \quad |E_u\rangle = -\sqrt{\frac{15}{5}}\left|\begin{array}{|c|c|c|}\hline 1&2&3\\\hline 4&5\\\cline{1-2}6\\\cline{1-1}\end{array}\right\rangle + \sqrt{\frac{10}{5}}\left|\begin{array}{|c|c|}\hline 1&6\\\hline 2&3\\\hline 4&5\\\hline\end{array}\right\rangle$$

are not eigenstates at. all. Instead, very special "broken tableau" states such as

$$\left|\begin{array}{|c|c|c|}\hline 1&2&3\\\hline 4&5\\\cline{1-2}\end{array}\uparrow\uparrow\uparrow\uparrow \quad \begin{array}{|c|}\hline 6\\\hline\end{array}\uparrow\downarrow\right\rangle = \sqrt{\frac{1}{3}}|A_{2u}\rangle + \sqrt{\frac{2}{3}}|E_u\rangle, \text{or} \left|\begin{array}{|c|c|c|}\hline 1&2&3\\\hline 4&5\\\cline{1-2}\end{array}\uparrow\uparrow\uparrow\downarrow \quad \begin{array}{|c|}\hline 6\\\hline\end{array}\uparrow\uparrow\right\rangle = \sqrt{\frac{2}{3}}|A_{2u}\rangle - \sqrt{\frac{1}{3}}|E_u\rangle$$

i.e. "mixtures" of A and E species are needed to describe the molecule.

Transformations and covrelations between the two types of states "pure" and "mixed" have been constructed for most types of clusters. Hamiltonian or energy material have been constructed in either basis and the eigenvalues and spectra are now being studied using the HP desk plotter. (See for example Figs 15-19 in Phys. Rev A24 pp 228-238) Hyperfine mixing first manifests itself in so-called "saturation crossovers". (See Figs. 6,9, and 10 on pp. 201, 204, and 205).

These results may be significant for at least three reasons. First, the collisional relaxation of SF_6 molecules will be influenced by the ability of single molecules to switch species more in one type cluster than in another. Secondly, the "breaking" of six-nuclei wavefunction into two or more parts (In the example it broke into an " equatorial" 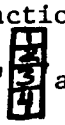 and "polar" 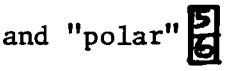 part.) provides a spectral structure which could be very useful for determining internal structural and dynamic details. Essentially, the rotating molecule is preparing itself in a nuclear magnetic resonance (NMR) configuration and the resulting spectra are generalized NMR patterns. Finally, the knowledge of the correct mixtures of A, E, and T species is certainly a prerequisite for future work on derived selection rules involving them.

Other work has progressed toward applications of the courser spectral structure. Fine structure clusters of excited vibrational states have been identified and a 16 mm laser system operating on the $\nu_2 \rightarrow \nu_2 + \nu_4$ transitions of CF_4 has been analyzed at Los Alamos. It turns out that laser action occurs for tight four-fold clusters. These developments open the possibility for using a complex spectra of a molecule to make a laser system which can then be turned

back on the same molecule to get very high resolution spectra. If this works out then the generalized NMR patterns will be more easily observed, and an important new spectroscopic field will be opened.

1. J. Bordé, Ch. J. Bordé, C. Salomon, A. Van Lerberghe, M. Ouhayoun. and C. D. Cantrell, Phys. Rev. Letters 45, 14 (1980).

BROKEN UNITARY TABLEAUS, ITINERANT NUCLEAR SPINS, AND SPONTANEOUS MOLECULAR SYMMETRY COLLAPSE

William G. Harter
School of Physics
Georgia Institute of Technology
Atlanta, GA 30332

Chris W. Patterson
Los Alamos Scientific Laboratory
Los Alamos NM 87545

Introduction

Applications of unitary group (U_m) and permutation group (S_n) representations have been the subject of two conferences organized by Professor Jürgen Hinze. The proceedings of the present conference mostly emphasize applications of unitary groups, while the those of the preceeding conference (1) mostly emphasize the permutation groups. A number of papers notably those of Wormer and Sarma in this volume, have reminded us of the inescapable relations between U_m and S_n groups. Many of the papers in these volumes have dealt with some number n of indistinguishable spin - ½ particles, for example, orbiting electrons, which may occupy some other number m of distinguishable states. The permutation group S_n of distinguishable particles serves as a symmetry group for the system Hamiltonian. The unitary group U_m corresponds to the set of all superpositions of the m states which preserve quantum amplitudes. The group U_m will be a symmetry group only if the m states remain degenerate in energy. Nevertheless, the U_m operations always commute with the S_n permutations so in some sense the two groups are symmetries for each other.

In this paper we shall consider n identical spin - ½ nuclei rotating inside an XY_n molecule. Berry and others (2) have noted similarities between this problem and the n-electron problem addressed throughout this volume. The correlation between levels of a rigid n-particle molecule and a completely non-rigid n-particle system were discussed by Berry (3) in the preceeding conference. Here we shall briefly point out some interesting detailed features of molecular levels which are due to non-rigidity and symmetry. These features came as a suprise to spectroscopists and theorists who first investigated high resolution spectra of molecules such as SiF_4, CF_4, OsO_4, and SF_6. (4) The explanations (5,6) of these features are providing a better framework for understanding detailed rovibronic dynamics of polyatomic molecules in general. (7-12)

These results are particularily exciting for this conference since this is a rare case in which group theoretical methods were needed from the very beginning to ellucidate unexpected physical phenomena. Furthermore, one expects similar features and phenomena to appear in high resolution gas phase electronic spectra of these and many other types of polyatomic molecules. When this happens it may add considerably to the importance of the electronic orbital calculations described in this volume.

1. Spectral Clustering and Induced Representations.

An example of modern high resolution spectra is shown by the ν_4:P(88) resonance $^{32}SF_6$ produced by Kim, Person, Seitz, and Krohn (13) in Fig. 1. The expanded view of high resolution spectra in Fig. 1 b-d shows the splitting of an angular momentum (J=88) peak into components labeled by octahedral (O_h) irreducible representations A_1, A_2, E, T_1, and T_2. Splitting into octahadral species is expected since the SF_6 molecule has octahedral symmetry. However, as shown in Fig. 1 b-c individual species are usually not well separated. Instead, they gang together into nearly degenerate clusters (T_1 T_2) (A_2 T_2 E), (T_1 T_2), (A_1 T_1 E), ... on the lefthand side and clusters (T_1 ET_2), (A_1 T_1 T_2 A_2),... on the right-hand side of Fig. 1b. Such clusters began to be noticed regularily in laser spectra and in computer eigenvalue calculations after the first SF_6 assignments were worked out at Los Alamos. Fox, Galbraith, Krohn, and Louck (4) first presented the clustering as a suprising and unexplained result in 1976, though related effects had been noted earlier in methane (CH_4) computer calculations by Dorney and Watson (14) and in atomic crystal field computer calculations by Lea, Leask, and Wolf (15). Dorney and Watson (14) had given a classical model which explained some properties of certain types of clusters. Since then a quatum theory (5-12) for spectral clusters has explained most of their properties. The theory is based upon a type of symmetry breaking which is quite the opposite to that which is normally discussed in applied group theory. Normally, the breaking or reduction of symmetry is associated with a splitting of degenerate levels of the original system. For example, if an octahedral system was perturbed by a C_4 or C_3 symmetric field, then its levels would split into singlets characterized by irreducible representations (irreps) of C_4 or C_3, respectively. The triplet octahedral level T_1 would split into C_4 levels (1_4), (0_4), and (3_4) under the C_4 field, and the C_3 field would split T_1 into (1_3), (0_3), and (2_3). This is written $T_1 \downarrow C_4 \sim 1_4 + 0_4 + 3_4$ and $T_1 \downarrow C_3 \sim 1_3 + 0_3 + 2_3$, respectively. These correspond to Zeeman splittings of a p-level into levels with magnetic quantum numbers m=1,0, and -1. The notation (3_4), for example, simply means m=3 modulo 4, and we note that -1=3 modulo 4 or $-1_4=3_4$. A complete accounting of all C_3 and C_4 splittings are recorded in the rows of the following tables.

	0_4	1_4	2_4	3_4
$A_1 + C_4$	1	.	.	.
A_2	.	.	1	.
E	1	.	1	.
T_1	1	1	.	1
T_2	.	1	1	1

Table 1a Octahedral-Tetragonal Correlation Table $O_h \downarrow C_4$

	0_3	1_3	2_3
$A_1 + C_3$	1	.	.
A_2	1	.	.
E	.	1	1
T_1	1	1	1
T_2	1	1	1

Table 1b Octahedral-Trigonal Correlation Table $O_h \downarrow C_3$

The remarkable thing about these tables is that their columns, which correspond to induced representations $a_n \uparrow O$, give the octahedral irreps present in clusters shown in Fig. 1b-c. This is an example of the other type of symmetry breaking which increases degeneracy. It unsplits or clusters levels rather than splitting them. It is appropriate to call this *internal* or *spontaneous symmetry breaking* since it is analogous to similarly named effects in solids and in high energy physics. Spontaneous symmetry breaking occurs when a system appears to collapse into a form which has a lower symmetry than that of the system Hamiltonian. This is a rather subtle quantum effect and it should be distinguished from the ordinary symmetry breaking in which the symmetry of the Hamiltonian is reduced by a perturbation. Jahn-Teller effects are examples of spontaneous symmetry breaking.

In the case of the octahedrally coordinated SF_6 molecule the centrifugal distortion causes the octahedron to collapse into less symmetrical shapes. The clusters on the left-hand side of Fig. 1b belong to octahedrons which have chosen to rotate on four-fold symmetry axes and have become distorted into a C_4 symmetrical shape. The octahedron has six equivalent four-fold axes (±x, ±y, ±z) corresponding to the subgroup C_4 and five cosets of C_4 in the octahedral O group. If an octahedron has collapsed completely into a C_4 symmetric top then a good quantum number would be the angular momentum n_4 around a particular C_4 axis which it has chosen. Strictly speaking the correct quantum label would be n_4 modulo 4 = (0, 1, 2, or 3) corresponding to C_4 irreps 0_4, 1_4, 2_4, or 3_4, respectively. In Fig. 1b the highest n_4 value is 88=0 modulo 4, i.e., the total angular momentum of the rotor (N=88) in the P(88) transition. (Vibrational angular momentum has been reduced by one quanta in all P(88) transitions, but the rotor momentum (N=88) and components (n) remain unchanged. Effects of vibrational momentum are treated in Refs. 8 and 10.) On the right-hand side of Fig. 1b several peaks are labeled in a similar way by irreps 0_3, 1_3, and 2_3 of C_3, corresponding to angular momentum n_3=88(=1 mod 3), 87=(=0 mod 3), 86=(=2 mod 3), and so forth around three-fold symmetry axes.

Fig. 1 High Resolution Anatomy of a ν_4 Transition in SF_6.
(a) Rotational Structure, and (b) Rotational *Fine Structure* of the P(88) Transition. (Fourier transform and infrared laser diode spectrum by K. C. Kim, W. B. Person, D. Seitz, and B. J. Krohn J. Mol. Spectrosc 76 322 (1979)). Rotational structure on the right-hand side is designated by P(N) where N is the angular momentum quantum of the SF_6 rotor before the transition. P means that the total angular momentum J=N+l(vib) of the molecule is one unit less (J=N-1) after the transition. The fine structure is divided into two groups of lines which are clusters of A, T, and E species. The sixteen or seventeen clusters on the left-hand side of P(88) correspond to rotation around four-fold symmetry axes, while the seven clusters on the right-hand side correspond to rotation around three-fold symmetry axes of the SF_6 octahedron. (c) *Superfine Structure*. The splitting of the four-fold and three-fold clusters depends strongly on the value of the components n_4 and n_3, respectively, of angular momentum on the four and three fold axes. If the splitting of a cluster is greater than about 1o kHz then the individual species may maintain their identity, and each has a well defined *Hyperfine Structure* (c). (See for example Fig. 4). These are called case 1 clusters. If the cluster splitting or superfine structure is less than the hyperfine splitting then the cluster belongs to case 2, and the A, T, and E species may become strongly mixed. (d) *Super hyperfine Structure*. In the extreme case 2 clusters the nuclear spins become oriented with respect to the octahedral frame. They may then give rise to spectral structures that are similar to NMR spectra in solids. (See Figs. 6, 8, and 9).

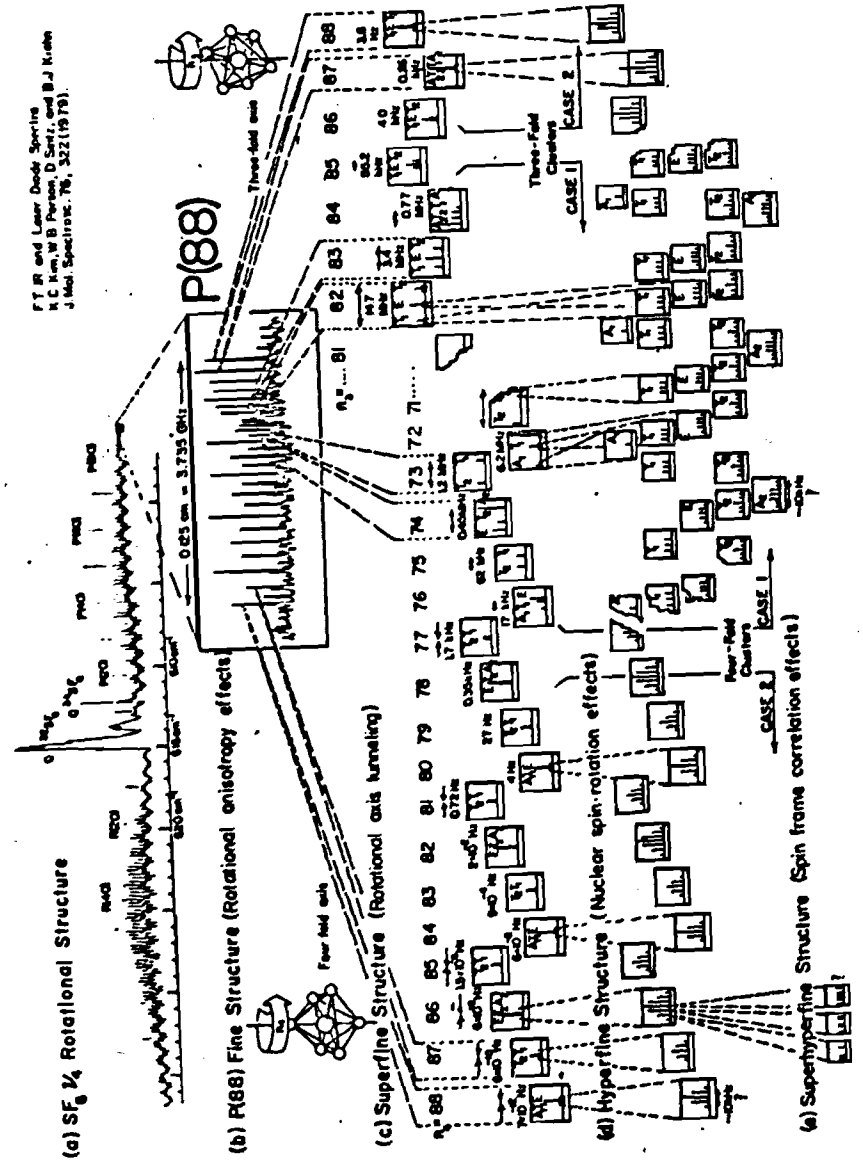

There are eight three-fold C_3 symmetry axes and six four-fold C_4 symmetry axes. The three-fold clusters $(n_3=88_3=1_3)+0=T_1+E+T_2$, $(87_3=0_3)+0=A_1+T_1+T_2+A_2$, etc., which appear on the right-hand side of Fig. 1b are derived from columns of Table 1b. Each cluster corresponds to eight rotational states in all. (Note that A_1 and A_2 denote singly degenerate octahedral irreps, while E and T_1 (or T_2) denote doubly and triply degenerate irreps, respectively.) In other words, there is one cluster state for each equivalent symmetry axis. Similarly, the clusters $(n_4=88_4=0_4)+0=A_1+T_1+E$, $(87_4=3_4)+0=T_1+T_2$, $(86_4=2_4)+0=A_2+T_2+E$, and so forth, are derived from the columns of Table 1a and appear on the left-hand side of Fig. 1b. Each cluster corresponds to six rotational states based upon six equivalent four-fold symmetry axes of rotation.

The construction of axial rotation states belonging to octahedral(A_1, T_1, E, T_2 A_2) labels requires some group theory and quantum mechanics of angular momentum. (12) However, the dynamics of one of the clusters, namely, $(0_4:A_1+T_1+E)$ can be visualized by appealing to classical and quantum analogies pictured in Fig. 2a and b, respectively. The quantum analogy involves a single particle tunneling between six potential valleys on an octahedral "planet" pictured in Fig. 2b. This in turn is analogous to six octahedrally coupled classical oscillators pictured in Fig. 2a.

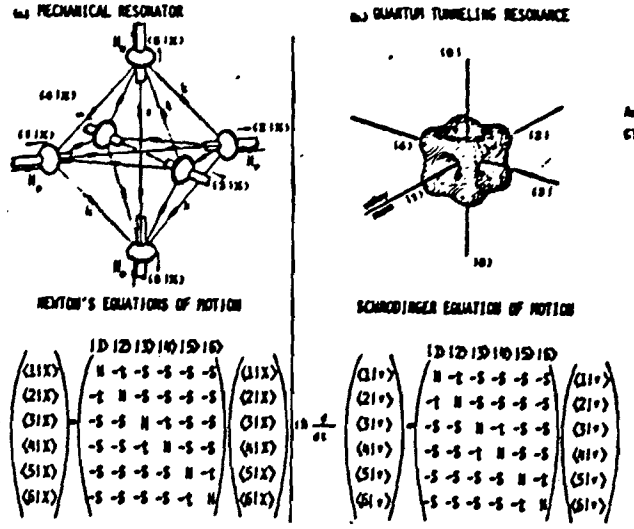

Fig. 2

Analogies for $0_4 \cdot 0$ Cluster States

(a) Classical analog involves six coupled oscillators

(b) Quantum analog involves particle capable of tunneling between six valleys. The angular position of the particle plays the role of the N-vector of angular momentum in the molecular clusters.

The right-hand sides of the equations of motion of the classical and quantum systems have similar matrices. The eigenvectors and eigenvalues of the matrices will be the same for either case. However, note that the classical Newton's equations have $-(d^2/dt^2)$ while the quantum Schrodinger's equations have $(i\hbar\, d/dt)$ on the left-hand side. This means the classical eigenvalues give the squared frequency or energy spectrum while the quantum eigenvalues give the frequency or energy spectrum directly. The diagonal components (H) of the coupling matrices correspond to local frequencies or energies. In the absence of the off-diagonal coupling components either system would correspond to six uncoupled degenerate oscillators i.e. a six-dimensional isotropic oscillator. Coupling causes resonant interactions between the oscillators. The nearest neighbor quantum tunneling amplitudes between the octahedral valleys in Fig. 2b are represented by (-S) coupling components in the matrix. These are related to classical spring constants (k) in Fig. 2b according to $-S=k/2$. In the theory of molecular axis tunneling it turns out that the nearest neighbor tunneling amplitude (-S) is very small and the next nearest tunneling amplitude t is neglible. In the classical mechanical model t is represented by a cross connecting spring constant t as shown in Fig. 2a. (It happens that the local frequency of the classical oscillator depends on connecting springs (i.e. $H=H_0+2k+t$) as well as the local H_0. This should just be regarded as a defect of the model.)

Eigensolutions of coupling matrices such as these can be found a number of ways by using the global symmetry group G of the system. If detailed eigenvectors are desired one may use the G symmetry projection operators

$$P^{\alpha}_{ij} = (\ell^{\alpha}/oG) \sum_{g} D^{\alpha}_{ij}(g)\, g \,. \qquad (1)$$

where ℓ^{α} is the dimension of irrep D^{α} and oG is the order of group $G=(1,g,g',\ldots)$. Eigenvectors are obtained by applying P^{α}_{ij} to a local state $|1\rangle$ which would have been an eigenvector in the absence of coupling.

$$|e^{\alpha}_{i}\rangle = P^{\alpha}_{ij}|1\rangle \,/(N^{\alpha})^{1/2} \qquad (2)$$

Here N^{α} are normalization constants. The eigenvectors of the matrices in Fig. 2 are the following

$$|e^{\alpha}_{i}\rangle = \begin{array}{ccccccc} & A_1 & E & E & T_1 & T_1 & T_2 \\ i= & 1 & 1 & 2 & 1 & 2 & 3 \end{array} \begin{pmatrix} 1 & 1 & 0 & 0 & 0 & 0 & | \\ 1 & 1 & 0 & 0 & 0 & 0 & | \\ 1 & -\tfrac{1}{2} & \tfrac{1}{2} & 1 & 0 & 0 & | \\ 1 & -\tfrac{1}{2} & \tfrac{1}{2} & -1 & 0 & 0 & | \\ 1 & -\tfrac{1}{2} & -\tfrac{1}{2} & 0 & 1 & 0 & | \\ 1 & -\tfrac{1}{2} & -\tfrac{1}{2} & 0 & -1 & 0 & | \end{pmatrix} \begin{matrix} /\sqrt{6} & /\sqrt{3} & /\sqrt{2} & /\sqrt{2} & /\sqrt{2} \end{matrix} \begin{matrix} |1\rangle \\ |2\rangle \\ |3\rangle \\ |4\rangle \\ |5\rangle \\ |6\rangle \end{matrix} \qquad (3a)$$

with eigenvalues

$$H^{A1} = H-4S+t \qquad H^{E} = H+2S+t \qquad H^{T1} = H \quad t \qquad (3b)$$

Fig. 3 is an attempt to picture the eigenvectors. By neglecting (t) the eigenvalues predict a two-to-one splitting for $(A_1T_1):(T_1E)$. This is the beginning of the theory for the *superfine* structure of the O_4 clusters as sketched in Fig. 1c. Note how S or the cluster splitting (Most splittings are calculated but some are observable.) varies from cluster to cluster in Fig. 1c. The splitting drops from 6.2 megaHz for the n_4=72 cluster to about the same number of pico Hz for the n_4=88 cluster! The splitting is inversely proportional to the "half-life" of non-stationary or local rotational states. Note that this varies from fractions of microseconds to many thousands of years! (Of course, the hyperfine or nuclear spin structure (Fig. 1d) ends up playing an important role as we will explain later.)

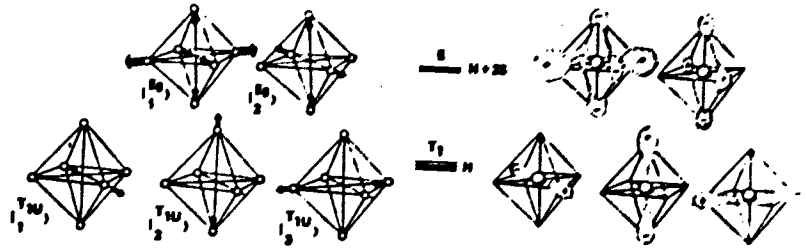

Fig. 3

Eigensolutions for Cluster Analogs. $P_4 \cdot P = A_1 \cdot T_1 \cdot E$

(a) Classical Eigenvectors

(b) Quantum Eigenmodes

The form of the eigenvalue spectrum makes the time behavior of non-stationary local states easy to predict. For example if we start at time $\tau=0$ with the localized state

$$|1\rangle = |e^{A1}\rangle /\sqrt{6} + |e_1^E\rangle /\sqrt{3} + |e_3^{T1}\rangle /\sqrt{2} \qquad (4)$$

then the quantum system evolves into the state

$$|1(\tau)\rangle = e^{H\tau/i\hbar}\left\{ e^{-4S\tau/i\hbar}\,|e^{A1}\rangle /\sqrt{6} + e^{2S\tau/i\hbar}\,|e_1^E\rangle /\sqrt{3} + |e_3^{T1}\rangle /\sqrt{2} \right\} \qquad (5a)$$

at time τ. (Here tunneling amplitude t is neglected.) It becomes completely delocalized at $\tau = \pi/2S$ which you might call its "whole life". At this time it has the form

$$|1(\pi/2S)\rangle = (|1\rangle - 2|2\rangle + |3\rangle + |4\rangle + |5\rangle + |6\rangle)/3 \qquad (5b)$$

Then it begins to roll back until it returns to state $|1\rangle$ again at $\tau=\pi/S$. Note that a non-zero t amplitude could prevent the state $|1\rangle$ from ever again being completely localized unless S was an integral multiple of t.

The local symmetries of localized states such as $|1\rangle$ determine the form of the induced representation they generate. The displacement vector $|1\rangle$ of the classical oscillator is invariant to C_4 rotations R_3, R_3^2, and R_3^3 by 90^0, 180^0, and 220^0 around the octahedral axis. In other words the state $|1\rangle$ is a basis of the (0_4) irrep of the octahedral axis. In other words the state $|1\rangle$ is a basis of the (0_4) irrep of subgroup C_4. This is equivalent to saying that the states $(|1\rangle, |2\rangle, \ldots\ldots, |6\rangle)$ span the induced representation $0_4\uparrow O$ of the octahedral group O induced by 0_4 of subgroup C_4. It also implies that projection $P^{\alpha}_{1,j}|1\rangle$ in Eq. 1 will yield an eigenstate only if sub index j is correlated with the local symmetry 0_4; i.e. $j=0_4$. This is possible only if irrep D^{α} contains irrep 0_4 of C_4.

$$D^{\alpha}(\text{of } O)\downarrow C_4 \sim \ldots \oplus 0_4 \oplus \ldots \qquad (6)$$

This line of reasoning leads to a simple proof of the Frobenius Reciprocity Theorem i.e. it explains why the columns of correlation tables yield induced ($\uparrow$) representations and clustering if the rows give subduced ($\downarrow$) representations and level splittings. It also leads to very simple coset factorization of eigenvalue and matrix element formulas. It is similar to double coset procedures of Frame and Seligman described in the preceeding conference (15).

The quantum model is not so restricted to having only 0_4 local symmetry in the way that the classical model is. The clusters $1_4\uparrow O$, $2_4\uparrow O$, or $3_4\uparrow O$ occur if the local wavefunction has angular momentum 1,2, or 3, respectively, modulo four. Similar analysis may easily be done for clusters based on local states on three-fold as well as two-fold and one-fold symmetry axes. These all may occur at high angular momentum, and they depend on the "geography" (16) of the Coriolis or centrifugal distortion potential and the initial conditions of the quantum state.

2. Tableau States and Permutation Clusters.

A more elegant and complete description of the octahedral XY_6 molecules uses the full unitary and permutation group algebra. The (full) octahedral $O(O_h)$ group of twenty-four (forty-eight) operations is just a small subgroup of the group S_6 of $6!=720$ permutations of the six identical Y-nuclei. Here is a case where the molecules appear to have suffered severe spontaneous symmetry breaking in order to become octahedrons. This means that each of the octahedral species (A_{1g}, A_{1u}, A_{2g},..... T_{1u}, T_{2g}, T_{2u}) is associated with an induced representation ($A_{1g}\uparrow S_6$, $A_{1u}\uparrow S_6$,..... $T_{2u}\uparrow S_6$), respectively, and a corresponding cluster of energy levels belonging to tableau labeled irreps of S_6. The tableau states contained in each cluster are indicated by entries in the columns of the $S_6\downarrow O_h$ correlation table. This given in Table 2 with some additional information: the associated nuclear spin tableaus for Bose (integral spin) and Fermi (half-integral spin) nuclei are shown.

For spin-½ (Fermi) nuclei we only consider the last four rows of the table for which the tableaus have two rows or less. The only octahedral molecules observed so far in high resolution laser spectra are hexaflourides for which the nuclear spin is one-half. However, a hexachloride molecule could have isotopes with spin-5/2 and require U(6) spin tableaus. Then all eleven rows of Table 2, would be used. For analyzing laser spectra of high spin molecules one might need a general tableau analysis such as Sarma and Rettrup have discussed in this volume. This would be particularily important when laser spectrometers can resolve hyperfine structure.

The first evidence of hyperfine effects in SF_6 were obtained by C. J. Borde et. al. (17, 18) using saturation spectroscopy. In this technique counter propagating laser beams are used in a way that virtually eliminates Doppler broadening. An example of a $1_3\uparrow O \sim T_1\oplus E\oplus T_2$ cluster at high resolution is shown in Fig. 4a, and a single A_2 line at ultra-high resolution is shown in Fig. 4b. Both these spectra show hyperfine effects but only the latter has a clear hyperfine splitting. To understand the A_2 spectra note that the A_{2u} column of Table 2 gives the following induced representation.

$A_{2u}+S_6 \sim$  (S=1) ⊕ 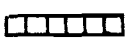 (S=3) (7)

In order words the A_{2u} peak corresponds to a cluster of tableau labeled states which belong to total nuclear spin (S=1) and (S=3), respectively. This cluster could be split by two effects. The first effect could involve nuclear permutation tunneling, i.e., nuclear permutations outside of the ocahedral subgroup. However, this astronomically small in a stable SF_6 octahedron. The second effect involves the tiny nuclear spin-rotation interaction. This splits the S=3 septet on top of the S=1 triplet as shown in Fig. 4b. (Notice that the three central peaks are about twice as high). To be strictly correct one should add the inversion partner A_{2g} to the A_2 cluster. (Inversion is included in the cosets of operations which are not exercised by the stable octahedral molecules.) However, the A_{2g} column of Table 4 is empty of spin-½ tableau correlation.

Nevertheless, inversion parity plays an important role in the analysis of most of the latest hyperfine spectra including the $1_3+0\sim T_1+E+T_2$ cluster in Fig. 4a. A tunneling matrix (5) similar to the one in Fig. 2b predicts that T_1-E and E-T_2 spacing should be equal as they appear to be in Fig. 4a. The hyperfine splitting of T_1, E, and T_2 is not quite resolved, but the line intensities are consistent with the permutation clusters predicted by Table 2. These are the following:

$T_{1g}+S_6 \sim$  (S=1) $\quad T_{1u}+S_6 \sim$ 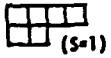 (S=1) (8a)

E_g+S_6 not possible with spin-½ nuclei $\quad E_u+S_6 \sim$ 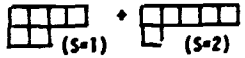 (S=1) (S=2) (8b)

$T_{2g}+S_6 \sim$ 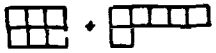 (S=0) (S=2) $\quad T_{2u}+S_6$ not possible with spin-½ nuclei (8c)

The ratios of the peak intensities $I(T_1):I(E):I(T_2)$ are consistent with the ratios of the number of spin components.

$$I(T_1):I(E):I(T_2)=(3+3):(0+3+5]):(1+5]+0) \quad (9)$$
$$= 6:8:6$$

Indeed, these statistical weight ratios were first derived using a more laborious

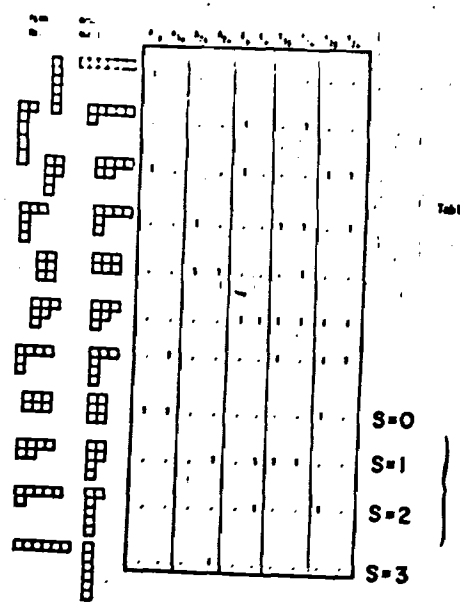

Table 2. Permutational - Octahedral Correlation Table $S_6 \sim O_h$. Only the last four rows are relevant for spin ½ nuclei.

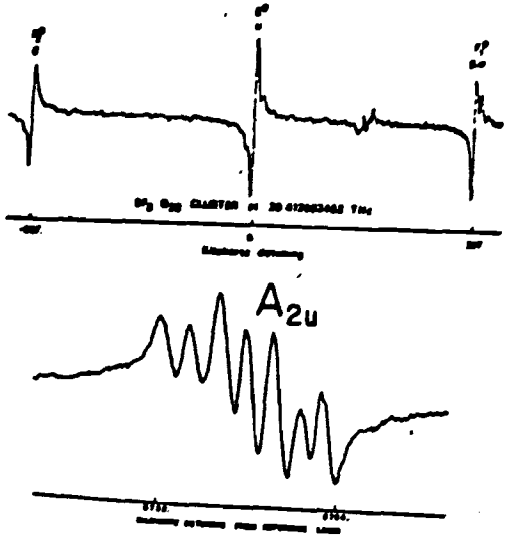

Fig. 4 Examples of Very High Resolution Saturation Spectra
(a) Cluster $1_3+0\sim T_1+E+T_2$ (Ch. J. Borde, M. Ouhayoun, V. Van Lerberghe, C. Salomon S. A. Awtillier C. D. Cantrell, and J. Borde, Ref. 18)
(b) Single A_2 Line (Ch. J. Borde, M. Ouhayoun, and J. Borde, J. Mol. Spec. 72, 344 (1978)).

procedure by Cantrell and Galbraith (19). However, their calculation was influenced by the Longuett-Higgins-Hougen molecular labeling scheme. This scheme makes parity analysis much more complicated than it needs to be (7) and can lead to erroneous conclusions. Indeed, when Ref. 7, containing Table 2, was submitted for publication in 1976 there was some controversy since it seemed to disagree with the results of Ref. 19. For example, Ref. 19 gives the summed weights of E_g and E_u as 8 and 8, respectively, while Table 2 gives 0 and 8, respectively. After publication of Ref. 7, Bordé (20) redid the analysis of SF_6 spin states. This work contains a sketch of both the methods of Refs. 7 and 19, though these works are not mentioned, and the power of tableaus is not fully realized. However, Bordé's results did corroborate those of Ref. 7. Still there was some suprise generated by the small "cross-over resonance" between E and T_1 in Fig. 4a, or, more specifically, by the lack of a similar cross-over resonance between T_2 and E. Weak saturation cross-over peaks can be expected to appear half-way between a pair of strong saturation peaks belonging to species which are mixed due to hyperfine interactions. (21) However, the symmetry analysis in Ref. (19) does not clearly indicate why there appears to be more hyperfine interaction between E and T_1 than there is between T_2 and E.

Bordé et. al., (18) found that this requires the parity assignments as given by Table 2. or more specifically by Eq. 8. There are no odd parity T_2 or even parity E hyperfine states and so the E-T_2 interaction is prohibited in spin-½ nuclei. However, the odd-parity E and T_1 states may interact. This is a good demonstration of the simplicity and power of tableau analysis where complete and correct labeling procedures were set up even before the theory of rotational clusters was formulated.

However, it is the presence of rotational clusters which makes hyperfine interactions important (12,22,23). The hyperfine spin-rotation interactions are small and nuclear spin-spin interactions are even smaller. In order for states belonging to different species such as E_u and T_{1u} to be strongly mixed by hyperfine interactions, they must have practically degenerate eigenvalues of the rotational (i.e. centrifugal and Coriolis) Hamiltonians. This happens whenever the cluster tunneling rate and splitting is less than the nuclear spin precession rates or hyperfine splittings. In other words when superfine (cluster) level structure is finer than hyperfine structure, states with different rovibronic species may be strongly mixed. These are called CASE 2 states and they are analogous to atomic jj-coupled states which are used when spin-orbit interactions have a dominant effect. For CASE 1 states the normal rovibronic species lables A_1, A_2, E, T_1, and T_2 and associated total nuclear spin tableaus are good quantum labels, and they are analogous to atomic LS-coupled states. For light molecules (e.g., CH_4) and low angular (J<10) momentum one expects to find only case 1 states except for extraordinary Hamiltonians (16) or (rarely) with accidental degeneracy. However, laser spectroscopy is showing that case 2 clusters are the rule rather than the exception for heavy XY_4 and XY_6 molecules particularly in the ground vibronic or pure rotational levels. From Fig. 3.6 it appears that more than half of the vibrational states belong to case 2 clusters if we assume that hyperfine splittings are tens of KiloHz. Case 2 clusters require a more general tableau labeling and this is discussed in the following sections.

3. Nuclear Spin Interactions in Clusters

The labeling of case 2 hexafluoride molecular states is first done using tableaus of S_6 and U(6) and then by subgroup chains appropriate to each type of cluster. Here examples involving molecules rotating on four-fold symmetry exes will be sketched briefly. An octahedral molecule rotating around a four-fold symmetry axis is pictured in Fig. 5.

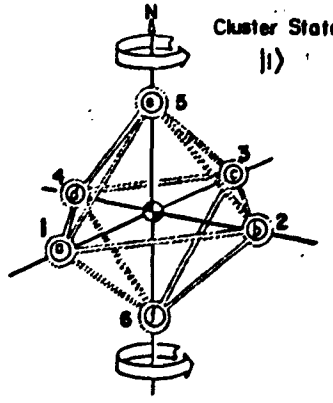

Fig. 5 SF_6 Molecule Rotating Around a Four-fold Symmetry Axis. Labeling of case 2 four fold cluster state depends on which nuclei (a,b,...,f) are in which single particle pockets (1,2,...,6).

Here one imagines six identical nuclei labeled a through f. Each nucleus may occupy any one of six "pockets" or states labeled 1 through 6. This is somewhat similar to unitary electronic orbital theory. The particles are spin-½ nuclei which have S_6 symmetry, i.e. they are indistinguishable. The orbitals are localized position states which are bases of U_6 and may be distinguishable. In the case of Fig. 5 states numbered 5 and 6 are distinguished by having nuclei localized on the axis of rotation while nuclei in states 1 through 4 are being thrown around in circle by the molecular rotation. Note that the numbering of the unitary states is not the same as the numbering of positions in Fig. 2. Also, in Fig. 5 we have six particles capable of occupying six positions, while in Fig. 2 one particle or one angular

momentum vector is capable of occupying six positions.

The molecular rotational cluster state

$$|1\rangle = \left| \begin{matrix} N & 1 \\ m & n \end{matrix} \right\rangle \qquad (10)$$

corresponds to $|1\rangle$ in Fig. 2. It has nucleus a in state 1, nucleus b in state 2, and so forth as shown in Fig. 5, with total rotational momentum N and body component $m=n_4$. The other cluster states $|2\rangle$, $|3\rangle$,...., and $|6\rangle$ in Fig. 2 correspond to octahedral rotations for which the N vector or the rotation axis is localized in one of six directions relative to nuclear octahedron (abecdf). However, the octahedral rotations are but a subgroup of all permutations of nuclei s,b,....,f relative to the octahedral pockets (125346) in Fig. 5. (Remember, pocket 5 is defined to be the one with the N-vector).

Here we are using a rather restricted unitary algebra since we never have more than one particle in given orbital state and no more states than particles. This is adequate for SF_6 molecules in stable configurations. However, one can imagine other situations involving dissociation, Berry rotation, dynamic Jahn-Teller effects, and chemically reactive scattering where a more general application of unitary basis would be needed.

However, all the 6! permutations in S_6 including inversion and all octahedral operations are part of this quantum theory. The relation between permutational tableau states and ordinary molecular symmetry operations is shown for XY_3 and XY_4 molecules in Refs. (7) and (23). For four-fold clusters one needs transformations between S_6 tableaus and states labeled by the octahedral subgroup chain $O_h > D_{4h} > D_{2h}$. These are given in Table 3, and derived in Ref. (24). Coset factorization helps to greatly to reduce the calculation needed to obtain these tables. Two examples from Table 3 are the states labeled (6,0) A_{2u}, B_{1u} and (5,1) E_u, B_{1u} which we will need later.

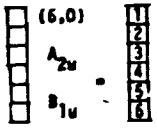

(11a)

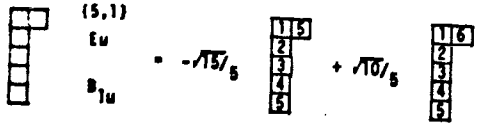

(11b)

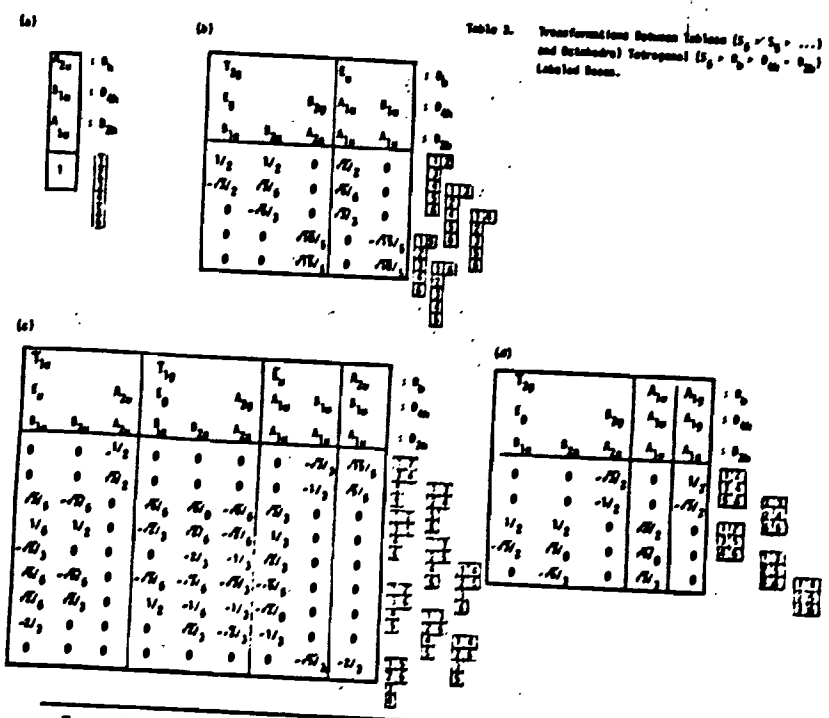

Table 3. Transformations Between Tableaux ($S_6 \supset S_5 \supset \ldots$) and Octahedral Tetragonal ($S_6 \supset D_{4h} \supset D_{2h}$) Labeled Bases.

To satisfy the Pauli Principle, each octahedral tableau state must be associated with a conjugate spin tableau corresponding to a definite total nuclear spin. For example, the state

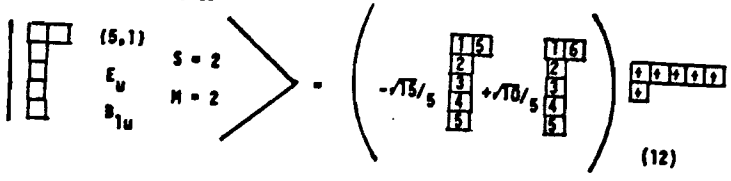

(12)

has orbital label (E_u(for O_h), B_{1u}(for D_{4h})) and spin angular momentum and component S=2 and M=2, respectively. It is instructive to expand these states in terms of Slater determinants. The M=2 states are shown in Table 4.

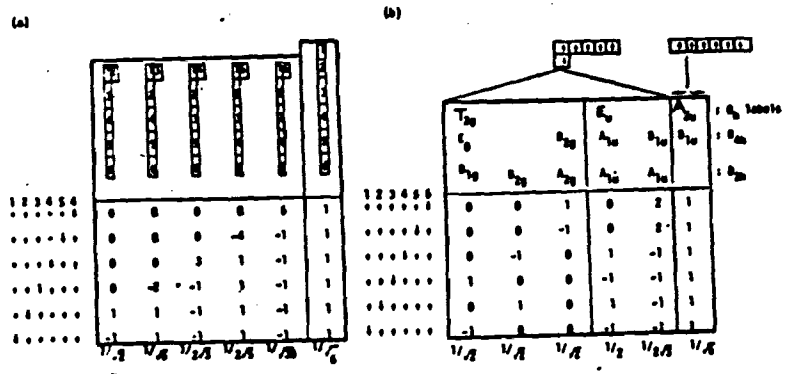

Table 4. Transformations between Slater determinant and (a) $(S_\zeta, S_\eta, \ldots)$ bases, (b) $(\Phi_a, \Phi_{2a}, \Phi_{2b})$ bases.

The states for all M are derived in Ref. (24) using the tableau assembly formula (25, 26). One should note that the columns of all such transformations can be written entirely using integers with a normalization factored out. One should also note the similarity between the columns of Table 4b and the tunneling eigenvectors given in Eq. (3a) or Fig. 3. For example the state

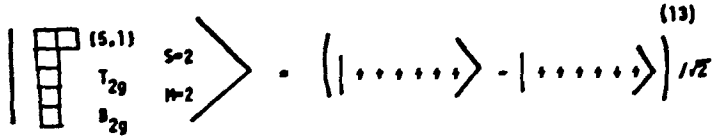

(13)

is analogous to the $\left|{}^{T_{1u}}_{2}\right\rangle$ state in Fig. 3b. Here one down-spin (↓) is capable of attaching itself to one of six octahedral nuclei while the other five have up-spin (↑). So now we see another analogy to the octahedral (A+T+E) tunneling cluster model in Fig. 3b. Nuclear spin exchange between adjacent octahedral vertices is analogous to tunneling of nuclei or the resonant switching of nuclear axes of rotation. One can think of spin exchange as the tunneling of a quasi-particle which might be called a "domon" from site to site. When strong case 2 conditions exist so that nuclear axis tunneling is prohibited by centrifugal forces, then the only tunneling mechanism open is spin-exchange or "domon" tunneling.

In case 2 conditions another effect called tensor spin-rotation interaction may be important. Nuclei which are moving faster may contribute more spin-rotation energy. The nuclei in states numbered 1 through 4 in Fig. 5 are moving faster than the ones in pockets 5 and 6 on the axis. The pseudo-Hamiltonian

$$H_{tsr} = N_z((6a+4)(S_z(1)+S_z(2)+S_z(3)+S_z(4)) + 4(S_z(5)+S_z(6))) \qquad (14)$$

for tensor spin-rotation depends on an anisotropy factor (a), the spin component $S_z(p)$ of the nucleus in position p and the body component of the molecular angular momentum $\langle N_z \rangle = n_4$ on the four-fold axis. A plot of the tensor energy $\langle H_{tsr} \rangle$ vs. the tensor anisotropy parameter (a) is given in Fig. 6.

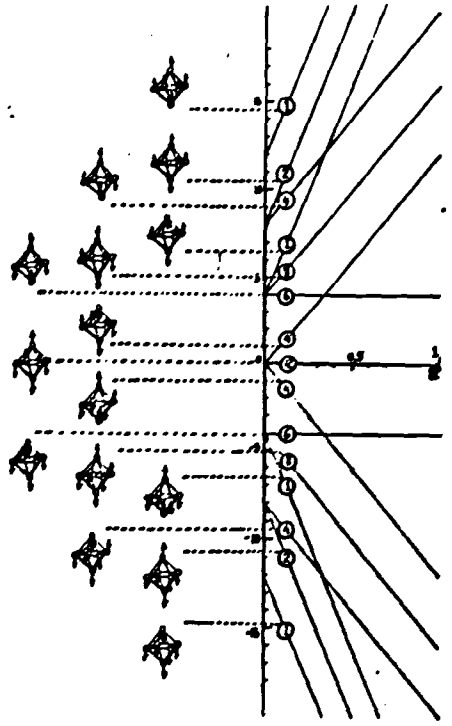

Fig. 6 Plot of Semi-classical Tensor Spin Rotation Levels for Octahedral-Tetragonal Case 2 Cluster States. The quantity (a) is a measure of the relative strength of tensor vs. scalar interaction. It is a measure of the difference between spin (↑) vs. (↓) energy of nuclei located on the rotational axis (in states 5 and 6) and those on the equator (in states 1 and 4).

If you disregard the Pauli principle the number of different spin states for each energy is shown by the circled numbers. Some examples of these spin states are sketched next to the numbers. The six "one-downon" or M=2 states correspond to the numbers ② and ④ near the top of the figure.

The approximate "one-downon" spin Hamiltonian matrix is represented in Table 5a in the Slater determinant basis and in Table 5b in the $(S_6 \supset O_h \supset O_{4h})$ tableau basis.

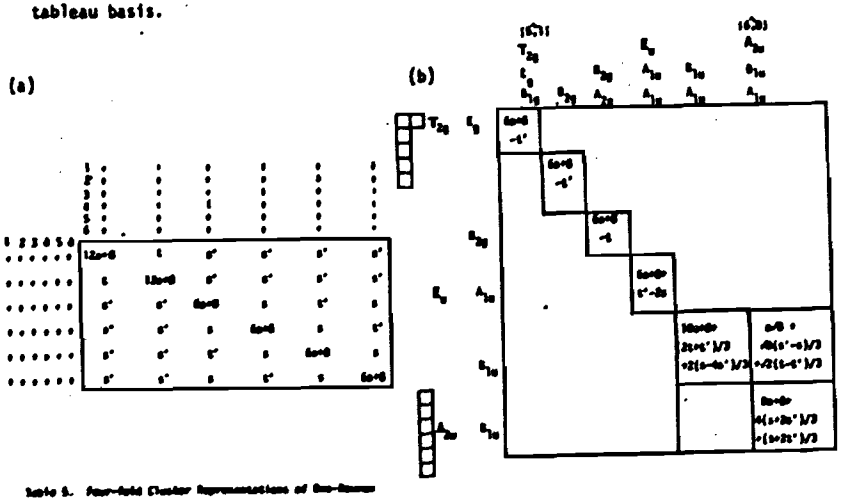

Table 5. Four-fold Cluster Representations of One-Downon Hyperfine Hamiltonian (a) Slater determinant basis (b) Tetragonal basis.

The Slater representation contains the values of the tensor operator on the diagonal. It also has off-diagonal nearest-neighbor tunneling amplitudes s and s' for tunneling transverse to the axis (e.g. $1 \rightleftarrows 2$, $2 \rightleftarrows 3$, etc) and along it (e.g. $1 \rightleftarrows 5$, $2 \rightleftarrows 6$, etc), respectively. Finally, cross tunneling parameters t for a $5 \rightleftarrows 6$ exchange along the axis and t' ($1 \rightleftarrows 3$ or $2 \rightleftarrows 4$) exchanges are included. The tunneling amplitudes are analogous to those in matrices of Fig. 2b with one difference; four-fold cluster rotation breaks the spin pseudo-Hamiltonian down to O_{4h}. The tableau representation in Table 5b is obtained by transforming Table 5a with the matrix in Table 4b. Note that a two-by-two matrix is left between the O_h species A_{2u} and E_u. This representation will not be diagonal unless the nuclear spin quantities (s-s'), (t-t'), and (a) are zero. This corresponds to one of the simplest examples of hyperfine mixing in SF_6.

4. Spinor Tableau Labeling of Tensor Eigenstates

We shall use the simple example of $A_{2u} - E_u$ mixing to show how tableau factorization leads to case 2 eigenvectors when the tensor parameter (a) dominates in cluster bases. This factorization uses the orbital tableau assembly formula (27) given by Fig. 7.

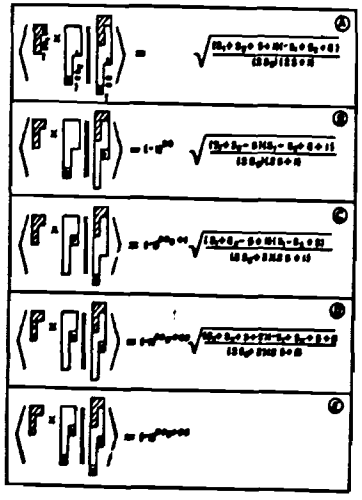

Fig. 7 Orbital Tableau Assembly or Factoring Formula. Subduction coefficients for $[\nu] \downarrow [\nu_1] \times [\nu_2]$ are found by successive removal of boxes with highest state numbers from tableaux $[\nu_2]$ and $[\nu]$. Each "removal" gives a factor in terms of conjugate total spins S_1, $S_{2'}$ and S, depending on where the highest states a are located (Cases A-E). All of the numbers in the formulas refer to the condition of the tableaux just before the boxes containing a are removed. Subduction coefficient is zero unless the tableau of $[\nu]$ contains the tableau of $[\nu_1]$ as indicated by the shaded area.

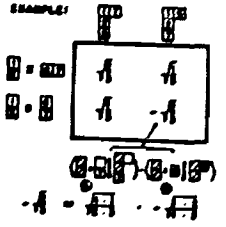

For example, this formula gives the following factorizations,

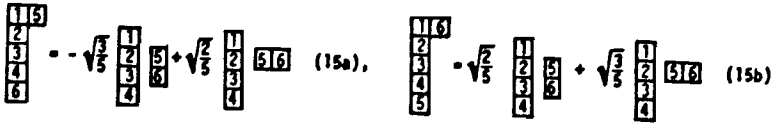

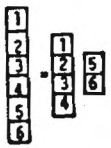

(16)

Substituting these into Eqs. 11 a,b yields the following simple factored expressions for A_{2u} and E_u orbital states.

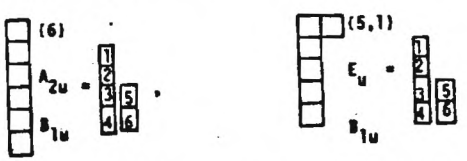

(17)

(This suggests that an easier way might exist for computing Table. 3). By attaching the appropriate spin tableau states with Clebsch Gordan coefficients one obtains appropriate spin states belonging to M=2.

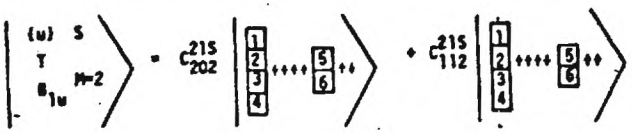

(18a)

Two examples are given.

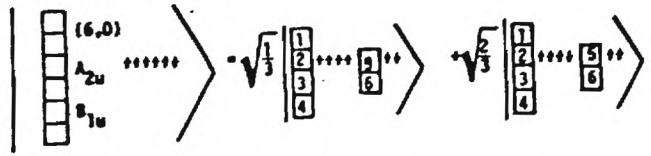

(18b)

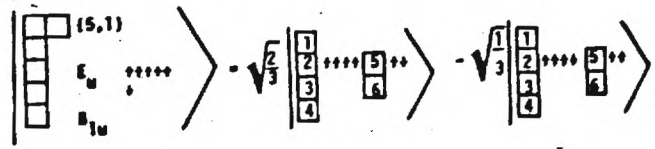

(18c)

...tation in the broken tableau basis

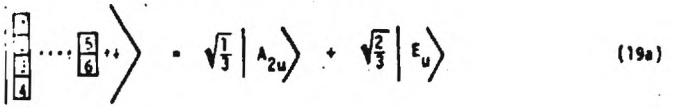

(19a)

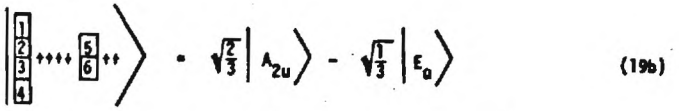

(19b)

of the B_{1u} submatrix of Table 5b takes the following form.

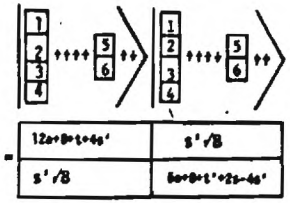

(20)

$12a+8t+4s'$	$s'\sqrt{8}$
$s'\sqrt{8}$	$8a+8t'+2s-4s'$

This is diagonal if s' can be ignored in comparison to a. The correlation of all the "one downon" (M=2) levels is drawn in Fig. 8 between the extremes of (a=0=t) and large (a).

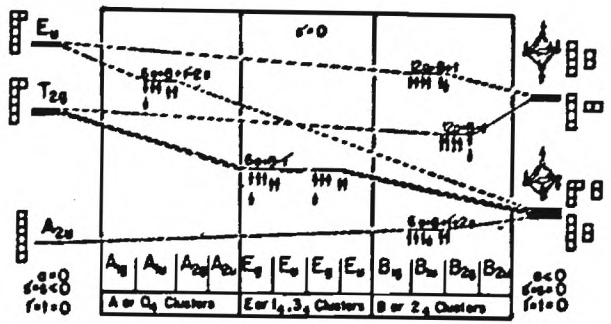

Fig 8. Case 2 Energy Level Correlations for a One-Downon Subclusster. The right-hand side corresponds to a dominant tensor spin-rotation parameter (a), while the left-hand side corresponds to dominant spin exchange tunneling parameters (s=s').

The effect of large (a) on case 2 clusters is to "divorce" the permutational wavefunction into particles which stay on the axis of rotation and those which move around off the axis. This sort of permutational divorce is a very important form of spontaneous symmetry breaking. It happens in photoionization processes as sketched by Patterson, Harter, and Schneider in this volume. It seems to play a part in allowing one to truncate closed shells. Indeed, without it, every problem in the world be a very-many-body-problem. It is doubtful that our society could exist as we know it if everyone's electrons and nucleons were permutationally correlated. Indeed, spontaneous symmetry collapse is not the end of the world but rather the beginning of it!

For SF_6 and related molecules the permutational divorce and corresponding large hyperfine mixing is related to the spontaneous rotational symmetry breaking. The rotational cluster eigenvalues for the 2_4+0~ A_2+T_2+E are the same as the ones in Eq. 3b for A_1, T_1, and E_1 namely, H-4S, H, and H+2S, respectively. To compute case 1 levels these eigenvalues need to be added to the appropriate diagonal positions of a Hamiltonian matrix such as Table 5b. Case 2 corresponds to S being small compared to the hyperfine quantities a,s,s',t or t'. If S is large then the divorce game is over and the individual species A T and E will recover their case 1 identities and total nuclear spin will be a good quantum number again.

Fig. 9 shows a full correlation between A_2+T_2+E levels for case 1 conditions on the right-hand side and case 2 conditions on the left-hand side. The case 2 levels collect into subclusters of zero dounon (N=3), one dounon (N=2), two dounon (N=1) levels as they appear in Fig. 6 for a=1/6. The levels within these subclusters would be effected by spin exchange or dounon tunneling (Recall Fig. 8) and they could yield many interesting spectral structures. In Fig. 1e we refer to these possible transitions as *superhyperfine* structure.

The details of the wavefunctions for these and other cluster states we give in Ref. 24. Also the problem of frame transformation of spin angular momentum between laboratory and molecular frames (7,23) is discussed. Finally, it is possible to understand the nature of transitions between case 1 and case 2 levels. This is important since the ground state pure rotational levels turn out to be mostly case 2 clusters. (18)

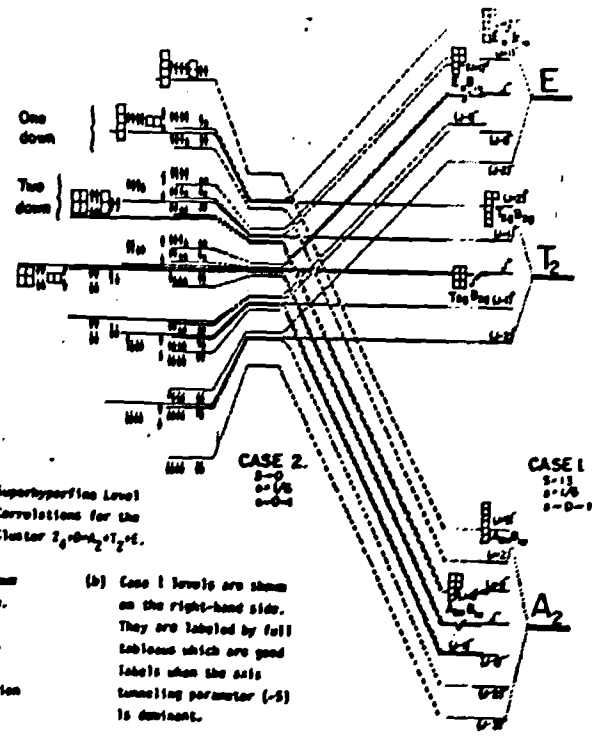

Fig 9. Superhyperfine Level Correlations for the Cluster 2_4+0~A_2+T_2+E.

(a) Case 2 levels are shown on the left-hand side. They are labeled by broken tableaux which are good labels when the tensor spin-rotation parameter (a) is dominant.

(b) Case 1 levels are shown on the right-hand side. They are labeled by full tableaux which are good labels when the axis tunneling parameter (-S) is dominant.

5. Conclusion

The combination of rapidly developing laser techniques and group theoretical methods opens up a tremendous new field for physicists, mathematicians, and quantum chemists to explore. New basic quantum phenomena are ripe for theoretical discovery or analysis and experimental verification. The unexpected possibility for the importance of nuclear spins in molecular dynamics needs further study, and it should not be confined just to spin-½ U(2) nuclei. Nuclei with spin 1 (U(3)) and higher may exhibit quadrupole effects in the cluster configurations. (28) The power of unitary and permutation group methods is only beginning to be used.

Rather than giving a long list of existing and future areas of development we shall attempt to give a "road map" of this field on the next page. We hope this will be amusing to some readers. At least it should convey the idea that we are having a lot of fun with this work, and we hope others will join us.

Acknowledgement

This work was supported in part by a grant from Research Corporation.

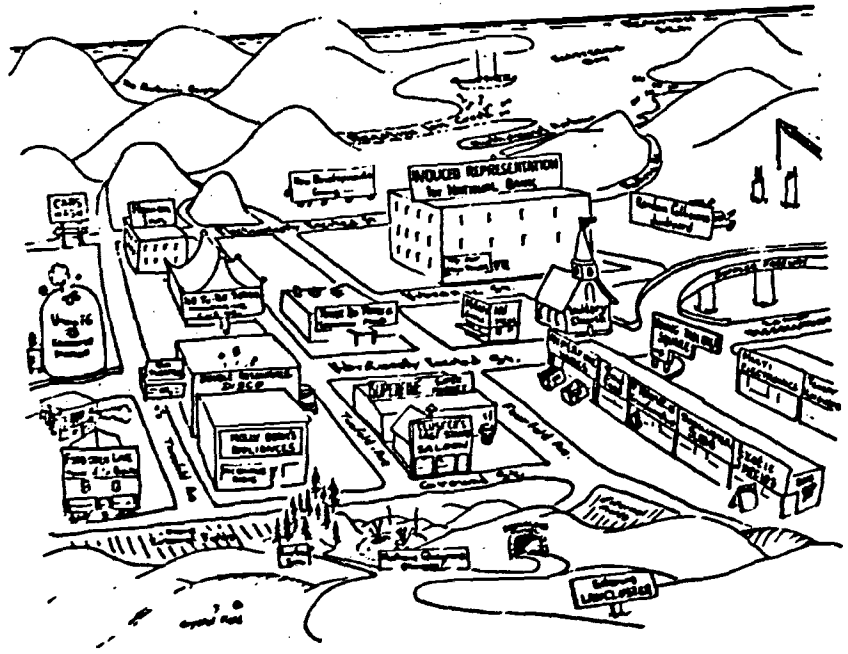

REFERENCES

1. J. Hinze (editor) The Permutation Group in Physics and Chemistry, Lecture Notes in Chemistry 12, (Springer Verlag 1979).
2. R. S. Berry, Revs. Mod. Phys. 32, 447 (1960); S. J. Dalton, J. Chem. Phys. 54, 4745 (1971); F. Amar, M. E. Kellman, and R. S. Berry, J. Chem. Phys. 70, 1973 (1979).
3. Ref 1., p. 92-120.
4. K. Fox, M. W. Galbraith, B. J. Krohn, and J. D. Louck Phys. Rev. A 15, 1363 (1977); R. S. McDowell, in Laser Spectroscopy III, edited by J. L. Hall and J. L. Carlsten (Springer Verlag 1977), p. 102.
5. W. G. Harter, and C. W. Patterson, Phys. Rev. Lett. 38, 224 (1977); J. Chem. Phys. 66, 4872 (1977); Int. J. Quantum Chem. Symposium No. 11, 479 (1977).
6. C. W. Patterson, and W. G. Harter, J. Chem. Phys. 66, 4886, (1977).

7. W. G. Harter, C. W. Patterson, and F. J. da Paixao, Revs. Mod. Phys. 50, 37 (1978).
8. M. W. Galbraith, C. W. Patterson, B. J. Krohn, and W. G. Harter, J. Mol. Spectros. 73, 475 (1978).
9. W. G. Harter, M. W. Galbraith, and C. W. Patterson J. Chem. Phys. 69, 4888, (1978).
10. W. G. Harter, C. W. Patterson, and M. W. Galbraith J. Chem. Phys. 69, 4896, (1978).
11. C. W. Patterson, M. W. Galbraith, B. J. Krohn, and W. G. Harter, J. Mol. Spectros. 77, 457 (1979).
12. W. G. Harter and C. W. Patterson, in Group Theoretical Methods in Physics edited by J. Ehlers et. al., Lecture Notes in Physics 94 (Springer Verlag (1979).
13. K. C. Kim, W. B. Person, D. Seitz, and B. J. Krohn, J. Mol. Spectros. 76, 322 (1979).
14. A. J. Dorney, and J. K. G. Watson, J. Mol. Spectrosc. 42, 135 (1972).
15. T. M. Seligman, Ref. 1, p. 178; J. S. Frame, p. 193.
16. W. G. Harter, and C. W. Patterson, J. Math. Phys. 20, 1453 (1979).
17. Ch. J. Borde', M. Ouhayoun, and J. Borde', J. Mol. Spectrosc. 73, 344 (1978).
18. Ch. J. Borde', M. Ouhayoun, A. Van Lerberghe, C. Salomon, S. Avrillier, C. D. Cantrell, and J. Borde', in Laser Spectroscopy IV, edited by H. Walther and K. W. Rothe, Springer Series in Optical Sciences, (Springer Verlag 1980).
19. C. D. Cantrell, and M. W. Galbraith J. Mol. Spectrosc. 58, 158 (1975).
20. J. Borde, J. de Physique Lettres 12, L-175, (1978).
21. C. J. Borde, G. Camy, and B. Decomps Phys. Rev. A20, 254, (1979); C. J. Borde in Laser Spectroscopy III edited by J. L. Hall, and J. L. Carlsten, Springer Series in Optical Sciences 7 (Springer Verlag, 1977) p. 121.
22. W. G. Harter, and C. W. Patterson, Advances in Laser Chemistry, edited by A. H. Zewail (Springer Verlag, 1978).
23. W. G. Harter, and C. W. Patterson, Phys. Rev. A19, 2277 (1979).
24. W. G. Harter, and C. W. Patterson, "Theory of Hyperfine and Superfine Levels in Symmetric Polyatomic Molecules II. Elementary Cases in Octahedral Hexafluoride Molecules", (submitted to Phys. Rev. A).
25. W. G. Harter, and C. W. Patterson, A Unitary Calculus for Electronic Orbitals, Lecture Notes in Physics 49, (Springer Verlag 1976) p. 139; Phys. Rev. A 13, 1067 (1976).
26. G. W. F. Drake, and M. Schlesinger, Phys. Rev. A 15, 1990 (1977). These authors have related assembly coefficients to Clebsch Gordan coefficients.
27. C. W. Patterson, and W. G. Harter Phys. Rev. A15, 2372 (1977).
28. See for example Fig. 29 p. 66 of Ref. 7.